Journal of Environmental Chemical Engineering 10 (2022) 108500

Contents lists available at ScienceDirect

Journal of Environmental Chemical Engineering

journal homepage: www.elsevier.com/locate/jece

Effects of the presence of isosaccharinate on nickel adsorption by calcium silicate hydrate (CSH) gels: Experimental analysis and surface complexation modelling

Tiziana Missana *, Miguel García-Gutiérrez, Ursula Alonso, Ana María Fernández

CIEMAT, Physical Chemistry of Actinides and Fission Products Unit, Avenida Complutense 40, 28040 Madrid, Spain

ARTICLE INFO

Editor: V. Victor

Keywords:
Nickel, Organic ligands
Adsorption
Radioactive contaminants
Hazardous waste

ABSTRACT

The presence of organics may enhance contaminant mobility; thus, the evaluation of radionuclide-organic-cement interactions is a topic of particular interest for the safety assessment of low-intermediate level radioactive waste (LILRW) disposals. The objective of this work is to analyse nickel adsorption on the most abundant phases of hydrated cement paste, calcium silicate hydrate (CSH), in the presence of isosaccharinic acid (Isa), the principal degradation product of cellulose under alkaline conditions. Two different CSHs were studied (Ca/Si ratios of 0.8 and 1.4) to cover a range of chemical conditions representative of different cement degradation stages. To gather information on the interactions in the ternary Ni/Isa/CSH system, batch sorption tests, electrophoretic measurements, and spectroscopic analyses (FT-IR) were combined. The presence of Isa at a concentration up to $1{\cdot}10^{-2}$ M slightly decreased the surface charge (−10 mV) of the two CSH phases analysed, and moderately affected Ni adsorption, causing a diminution of K_d(Ni) by less than 1 order of magnitude. To interpret the experimental dataset, surface complexation modelling was successfully used in this system for the first time. The modelling was based on a double layer approach, which accounts for the properties of the binary Ni/CSH system and includes the formation of Ni-Isa aqueous complexes as well as Isa adsorption on the CSH, under the specific chemical conditions generated by the solids.

1. Introduction

Nickel radioactive isotopes (^{59}Ni and ^{63}Ni) can be formed by neutron activation in nuclear facilities, and they are radionuclides (RNs) of concern in the frame of low- or intermediate-level radioactive waste (LILRW) because of their long half-life: 76,000 and 100 years, respectively [4].

In LILRW repositories, cements are widely used as containment/conditioning materials [11], and calcium silicate hydrates, CSH, are the most abundant hydration products and important sorbing phases. Their poorly crystalline structure, which is difficult to analyse with X-ray diffraction techniques, gives them the attributes of *gels* [12].

One of the principal characteristics of cementitious materials is that they generate hyper alkaline conditions that, in principle, are expected to favour adsorption and precipitation processes, which are considered the main mechanisms preventing contaminants from spreading in the environment, and thus acting as safety factors in hazardous waste repositories.

Nevertheless, in LILRW disposals, the presence of organic compounds is quite common. Materials such as papers, tissues or plastics are stored with radioactive waste, and the presence of chelates used for decontamination processes or of organic additives mixed with cements cannot be ruled out. The alkaline or radiolitic degradation of these organics can generate strong complexing agents able to form very stable aqueous complexes with RN [13], enhancing their solubility and/or preventing their retention on the immobile solid phases.

The presence of organics is one of the possible causes of the enhancement of contaminant mobility [20] and is an issue of environmental concern. Studies focused on a detailed understanding of all those mechanisms affecting adsorption, especially those that can limit it –thus making contaminants more mobile– are of broad environmental interest [2,21].

However, the role of organics in LILRW disposals is difficult to predict due to the shortage of studies on ternary systems (radionuclides, organics, cementitious materials) under representative chemical conditions. The role of organic ligands on contaminant retention can be

* Corresponding author.
E-mail address: tiziana.missana@ciemat.es (T. Missana).

https://doi.org/10.1016/j.jece.2022.108500
Received 2 May 2022; Received in revised form 22 August 2022; Accepted 24 August 2022
Available online 26 August 2022
2213-3437/© 2022 The Author(s). Published by Elsevier Ltd. This is an open access article under the CC BY-NC-ND license (http://creativecommons.org/licenses/by-nc-nd/4.0/).

described by "sorption reduction factors", SRF [18], but the interactions of organic ligands with RNs and solid materials, as well as their response upon a change in the chemical conditions, are complex to be analysed and still far from being elucidated or described in a mechanistic way [14]. Thus, modelling efforts are becoming increasingly important to support the evaluation of all the main involved processes in the long term.

The main aim of this study is to analyse the effects of the presence of isosaccharinic acid (Isa) on Ni adsorption on CSH phases and, for the first time, to interpret the experimental results by sorption modelling.

Isa ($C_6H_{12}O_6$) is of interest in the framework of LILRW disposals because it can be formed when cellulose is degraded by the calcium hydroxide present in hydrated cement pastes and has been found to be the main degradation product of cellulose under alkaline conditions [9, 19]. For this reason, this is the most studied organic in the frame of radioactive waste disposal.

Indeed, Isa presents the capacity to form aqueous complexes with RNs, which is especially important for tri- and tetravalent actinides [23] but also for divalent cations, such as nickel [15]. Due to the presence of Isa, and in a range of pH values from 10.5 to 12.5, Warwick et al. [24] estimated a solubility enhancement for Ni of more than 100.

Nevertheless, the application of mechanistic sorption models to explain the RN/Isa/CSH interaction is very scarce and non-existent for Ni.

In this study, we experimentally analysed the effects of the presence of Isa on Ni adsorption on CSH gels and performed sorption modelling based on previous results obtained in the Ni/CSH binary system [16], where Ni adsorption and precipitation processes were analysed as a function of the CSH Ca/Si ratio.

The formation of Ni-Isa aqueous complexes and the possible adsorption of the organic on the CSH surface were both additionally contemplated to explain the behaviour of the ternary Ni/CSH/Isa system.

To apply sorption modelling, complete thermodynamic databases for RN speciation and solubility and RN-organic complexation are needed. The most important revision of Ni thermodynamic data is included in the OECD-NEA thermodynamic database [6], and the best compilation thus far for RN-organic complexes is also provided by the OECD-NEA [13]. This updated volume did not provide thermodynamic data for Ni-Isa complexes. Therefore, for the Ni-Isa system, a recent study [10] proposed a revision of both Ni and Ni+Isa data, which will be considered here.

The importance of thermodynamic modelling as a tool for assessing RN behaviour under variable chemical conditions is stressed.

2. Materials and methods

2.1. CSH phases

Two CSH gels at two different Ca/Si ratios (0.8 and 1.4) were selected because they represent two different degradation stages of the cement, generate different initial chemical conditions, and show opposite surface charges: negative for CSH(0.8) and positive for CSH(1.4). The gels were prepared by mixing CaO (Aldrich, 99.9% purity) and SiO_2 (Aldrich 99,8% purity) in boiled and N_2-sparged deionized water (Milli-Q system, 18 MΩ) following a standard method, already detailed elsewhere [17]. The suspensions were prepared to a solid to liquid ratio of 10 g·L^{-1}; during and after the synthesis, they were maintained in a glove box under a N_2 atmosphere.

An aliquot of these suspensions was centrifuged (9500·g, 60 min), and the supernatant was analysed to measure pH and the Ca and Si aqueous content by plasma spectroscopy (VARIAN 735ES). The solids were left to dry under an anoxic atmosphere in the glove box to minimise carbonation and then analysed by attenuated total reflection Fourier transform infrared spectroscopy (ATR-FTIR) with a Nicolet iS-50 apparatus in the range of 400–4000 cm^{-1} (middle infrared) and scanning electron microscopy with energy dispersive X-ray spectroscopy (SEM/EDS).

2.2. Isosaccharinic Acid (Isa)

The isosaccharinic acid used for the experiments was obtained in sodium form after the synthesis of Ca(α-Isa)$_2$, from which the α-form of Isa is produced [13], using a standard methodology described elsewhere [15,23]. Basically, Ca(α-Isa)$_2$ is produced by mixing monohydrated lactose and Ca(OH)$_2$ under a N_2 atmosphere. Ca(α-Isa)$_2$ has very low solubility in water; thus, Ca is exchanged by Na with an exchange resin (Chelex-100 BioRad).

The final dried sodium α-Isa to be used in the experiments (we will call it Isa, for the sake of simplicity) was crushed and analysed by ATR-FTIR. The spectra, including the main identified peaks, are presented in Fig. 1 S of the Supplementary Material. The unique reference for infrared spectroscopy data for α-Isa (isosaccharinic acid, isosaccharinate) can be found in Brinkmann et al. [3], who analysed the material dissolved at different pH values (< 9) to analyse its aqueous speciation. The range of the Isa concentration used in the experiments varied from approximately 1·10^{-4} to 1·10^{-2} M.

2.3. Radionuclide

The radionuclide used was ^{63}Ni isotope supplied by Eckert & Ziegler Isotope Products in the form of $NiCl_2$ in HCl 0.1 M, carrier-free. The concentration of Ni used for sorption tests was 1.1·10^{-9} M. The RN activity in solution was measured with a liquid scintillation analyser Tri-Carb 4910 TR (Perkin Elmer) and using Ultima Gold™ as a scintillation cocktail. The uncertainty for the counting procedure is less than 2%, and the detection limit is approximately 5·10^{-12} M.

2.4. ζ-potential measurement

The ζ-potential of the CSH gels was measured by laser Doppler electrophoresis using a Malvern Zetamaster apparatus equipped with a 5-mW He–Ne laser (λ = 633 nm, scattering angle 90°). Electrophoretic measurements were carried out with the CSH suspensions diluted with their own contact solution to 1 g·L^{-1}. The solution used for dilution is obtained by filtering the initial suspension through a 200 nm filter.

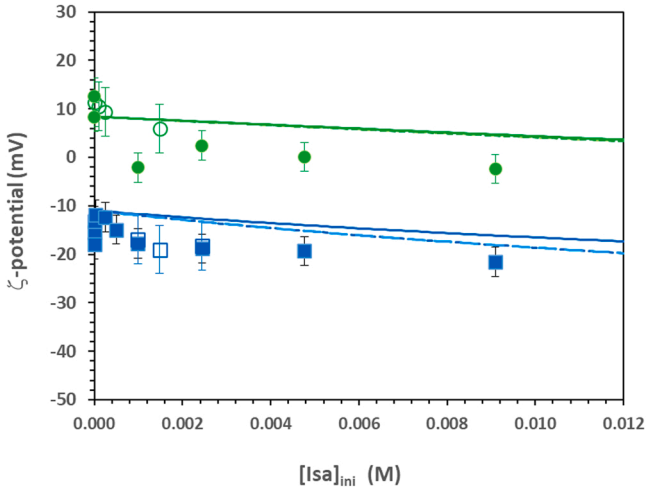


Fig. 1. : ζ-potential of the CSH phases *vs.* initial Isa concentration. Squares correspond to CSH(0.8) and circles to CSH(1.4); open points refer to measurements with the solid at a solid-to-liquid ratio of 10 g·L^{-1} and solid points to 1 g·L^{-1}. The lines correspond to the modelling of the surface potential of CSH (1 g·L^{-1}). Continuous line: no adsorption of Isa on the CSH; dotted line: Isa adsorption only in the weak site; dashed line: Isa adsorption on strong and weak sites.

Some point was measured at 10 g·L^{-1} for comparison.

Twenty millilitres of CSH suspension were distributed in polycarboxylate tubes, and different quantities of organic matter were added to each tube. The final pH was checked and readjusted to the initial value when necessary. The samples were stored in the glove box until their measurement. The value for the ζ-potential is taken considering the mean of at least five measurements. An image of the electrophoretic cell, where measurements are carried out, and of the Laser Doppler electrophoresis apparatus used is shown in Fig. 2S of the Supplementary Material. ζ-potential measurements were performed after 1 and 7 days upon organic addition and significant kinetics effects were not detected. The maximum variation in ζ-potential values was ± 3 mV for the measurements at 1 g/L and ± 5 mV for those at 10 g/L; the maximum observed error was taken for all the points.

2.5. Batch sorption experiments

Batch sorption experiments were carried out at a temperature of 22 ± 2 °C within a glove box under a N_2 atmosphere. Adsorption tests were carried out with a *low* Ni concentration (~10^{-9} M) because Ni solubility is limited under the alkaline conditions generated by the CSH phases, and we focused on the effect of the presence of Isa on Ni adsorption process.

The suspensions of the CSH phases (10 g·L^{-1}) were distributed in centrifuge tubes (10 mL), and then organic and Ni were added. The pH of the suspension was checked and readjusted to the initial value, if needed. After 1 week, the solid and liquid phases were separated by centrifugation (21255·g, 30 min) with a JOUAN MR23i centrifuge. Three aliquots of the supernatant were extracted from each tube for the analysis of the final Ni activity, and the distribution coefficient, K_d(Ni), was measured using the usual relation:

$$K_d(Ni) = \frac{[Ni]_{in} - [Ni]_{eq}}{[Ni]_{eq}} \cdot \frac{V}{m} \quad (1)$$

$[Ni]_{in}$ and $[Ni]_{eq}$ represent the initial and equilibrium Ni activity [cpm·mL^{-1}], m is the mass of the solid [g] and V is the volume of the solution [mL].

To evaluate Isa adsorption on the CSH phases, batch sorption tests were carried out with CSH at a solid-to-liquid ratio of 10 g·L^{-1} and Isa concentration of 5·10^{-5} - 1·10^{-3} M. The contact time between the solid and organic phases was 1 week. The separation of the solid from the liquid was performed by centrifugation (9500·g, 60 min), and the supernatant was analysed for the presence of residual aqueous organic matter, measuring the total organic carbon, TOC, using a TOC-V-CSH Shimadzu apparatus. The distribution coefficient for Isa, K_d(Isa), was calculated considering the initial value of TOC (corresponding to the added Isa) and the TOC value measured upon Isa sorption, the mass of the solid [g] and the volume of the solution [mL]. The background of TOC in the CSH suspensions and eventually released from vessels was checked in all the tests.

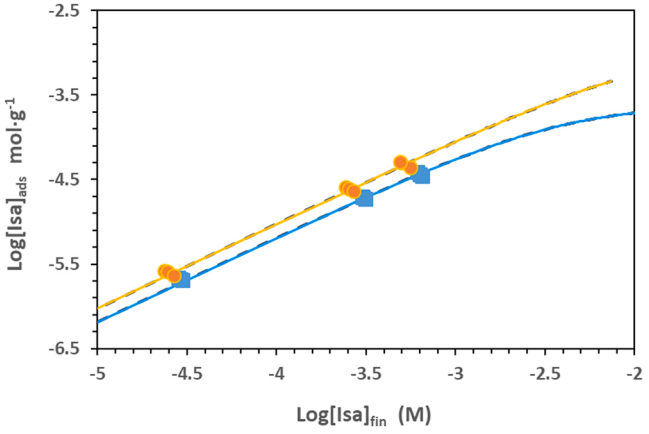


Fig. 2. Adsorption isotherms of Isa in: (■) CSH(0.8) and (•) CSH(1.4). Continuous and dotted lines correspond to the modelling of the experimental data considering the contribution of only weak or weak and strong CSH sorption sites, respectively.

2.6. Modelling description and database selection

The model used for describing the effect of Isa on Ni adsorption is based on a previous description of the CSH surface [17], which allowed fitting both the charge and the adsorption behaviour of the solid, and on the results obtained in the binary Ni/CSH system, concerning Ni sorption on CSH at different Ca/Si ratios [16].

The model is based on a double layer approach, where two different types of complexation sites (SiOH, *strong* and *weak*) are assumed to exist at the surface along with exchange sites (CaX_2) initially occupied by Ca. The reactions and parameters used to define the CSH surface are included in Table S1 in the Supplementary Material. To model Ni adsorption in the binary system, speciation calculations were carried out with the data provided in Table S2 in the Supplementary Material.

For the adsorption of Ni on the CSH gels, without organics, the following reactions were set:

a) Ni-Ca cation exchange: $X_2Ca + Ni^{2+} \leftrightarrow X_2Ni + Ca^{2+}$
b) Surface complexation of Ni^{2+}: $SiOH + Ni^{2+} \leftrightarrow SiONi^{+} + H^{+}$
c) Surface complexation of $Ni(OH)^{+}$: $SiOH + Ni(OH)^{+} \leftrightarrow SiONiOH + H^{+}$
d) Surface complexation of $Ni(OH)^{0}_{3}$: $SiOCa^{+} + Ni(OH)^{0}_{3} \leftrightarrow SiOCaNi(OH)_3$

Considering the very low solubility of Ni under alkaline conditions, only adsorption on the strong site (Si_sOH) was considered for Ni. The LogK of the surface complexes obtained from the abovementioned reactions (a-d) are summarised in Table S3 in the Supplementary Material.

To undertake the modelling of Ni adsorption in the presence of Isa, thermodynamic data from the OECD-NEA compilations are available for Ni and Ni+Isa [6] and [13]. However, González-Siso et al. [10] provided new experimental data for Ni and Ni+Isa under alkaline conditions and suggested some corrections to the previous databases, which will be considered here.

Model calculations were performed using the geochemical CHESS v 2.4 code [22] with the ThermoChimie database 10d [8], which basically gathers the values from the OECD-NEA databases. For the thermodynamic data of Ni and Isa accounted for the modifications recently proposed by [10].

3. Experimental results

3.1. Characterisation of CSH phases

The analysis of the supernatant of the CSH suspensions indicated a pH value of 10.28 ± 0.13 and Ca and Si concentrations of 44 ± 5 and 71 ± 10 mg·L^{-1}, respectively, for CSH(0.8); for CSH(1.4), the pH was 12.15 ± 0.10, and the Ca and Si concentrations were 335 ± 7 and 0.45 ± 0.10 mg·L^{-1}, respectively. The mean value for the N_2-BET surface area of the CSH gels analysed was 144 ± 40 m^2·g^{-1}.

The selected CSH phases initially present an opposite surface charge: the ζ-potential of CSH(0.8) is − 16 mV, and that of CSH(1.4) is + 10 mV. Considering the measurements obtained in different batches of CSH with the same theoretical Ca/Si ratio, these values may be subject to a variation of ± 5 mV. The CSH phases were analysed by SEM/EDS and FTIR, and their correct synthesis was verified. Fig. 3S in the Supplementary Material shows an example of the SEM/EDS measurements carried out for CSH phases. In general, the quantitative analyses for Ca/Si

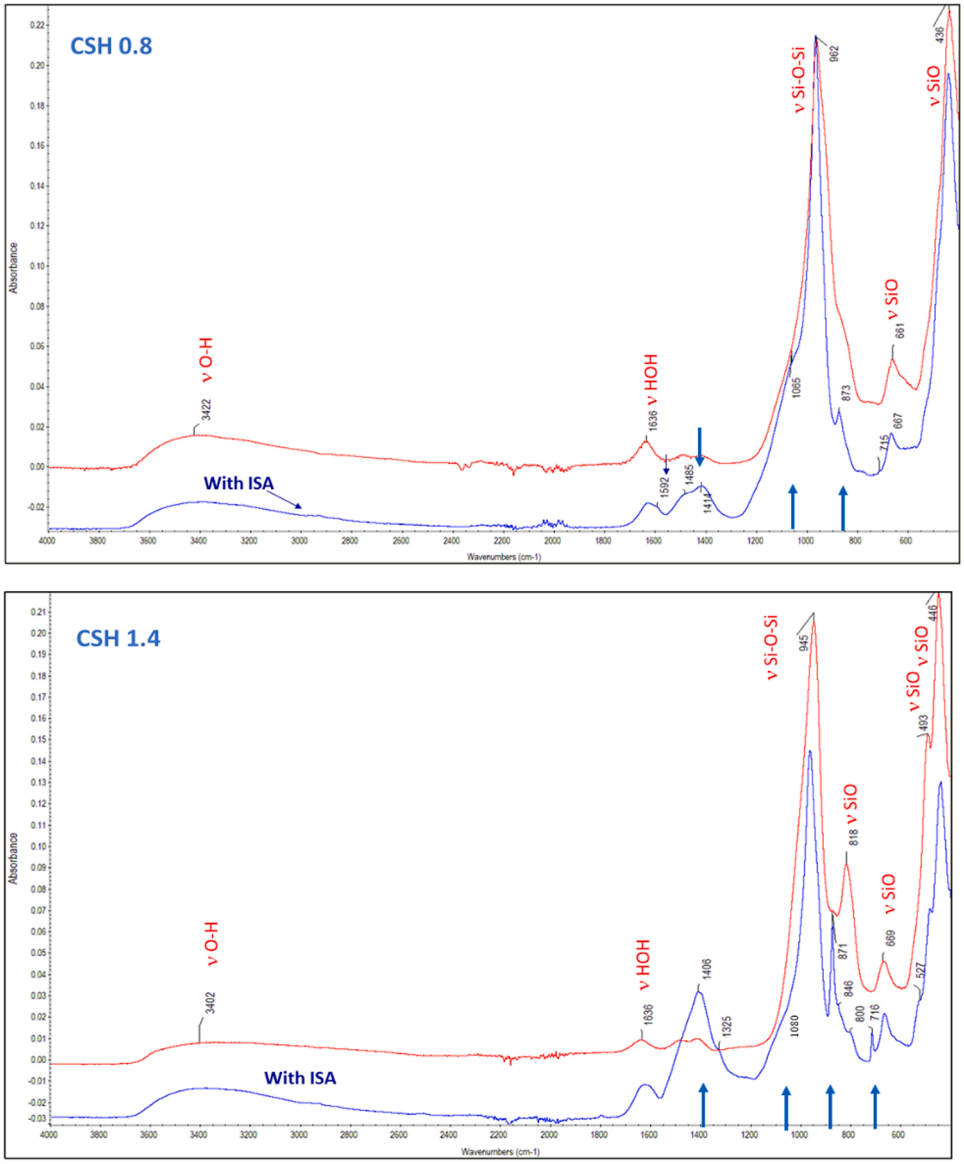


Fig. 3. : ATR-FTIR spectra of a) CSH(0.8) and b) CSH(1.4) before and after the adsorption of ISA ($9.1 \cdot 10^{-3}$ M).

determination obtained by SEM/EDS agree with the theoretical ratio.

3.2. Electrophoretic potential of CSH in the presence of Isa

Fig. 1 shows the ζ-potential of the CSH (0.8) and CSH (1.4) as a function of the increasing the initial Isa concentration, [M]. The presence of Isa, within the analysed concentration range, slightly affects the charge of both CSH phases, producing a net decrease of a maximum of 10–15 mV and being slightly higher in the CSH(1.4), even at the highest added Isa concentration.

3.3. Adsorption of the organics on the CSH

Sorption of the organic in solid materials can be an important process affecting the behaviour of the ternary system because adsorption of the organic reduces its concentration in the aqueous phase and its capacity to complex RN in the mobile aqueous phase.

The small effect produced by the addition of Isa on the CSH surface potential, as observed in Fig. 1, may be a first indication of a relatively weak interaction of the organic with the solid in terms of adsorption.

The experimental values for the distribution coefficients obtained for Isa (K_d(Isa)), in batch experiments by TOC measurements, were 64.5 ± 7.2 and 97.4 ± 10.6 $mL \cdot g^{-1}$ for CSH(0.8) and CSH(1.4), respectively.

These mean values were calculated considering the results obtained using Isa at different concentrations because, due to dispersion of data, no clear differences were detected as a function of the ISA concentration, and linear sorption was assumed. The Isa sorption isotherms are depicted in Fig. 2.

K_d values are not negligible, especially for the highest Ca/Si ratio; indeed, higher adsorption is expected for anions in CSH gels with Ca/Si > 1.2, due to their positive surface charge.

The distribution coefficients obtained in this work are higher (even if on the same order of magnitude) than other values previously published for Isa sorption on CSH phases. García et al., (2020) [7] determined the K_d (Isa) in CSH (0.8) and CSH (1.2) phases (at 20 and 50 $g \cdot L^{-1}$) and found higher Isa adsorption on CSH (1.2) (~ 70 $mL \cdot g^{-1}$) than on CSH (0.8) (~ 30 $mL \cdot g^{-1}$), confirming the same tendency of higher Isa adsorption in CSH with a higher Ca/Si ratio.

Androniuk et al. [1] investigated the adsorption of gluconate (anionic form of gluconic acid, $C_6H_{12}O_7$) on CSH phases and observed the same dependence of adsorption on the CSH Ca/Si ratio. Furthermore, from the linearity of the adsorption process from 10^{-5} to 10^{-3} M,

they concluded that a unique type (or a preferential) sorption site was responsible for gluconate uptake.

ATR-FTIR analysis was performed on the CSH gels after the adsorption of Isa at a concentration of $9.1{\cdot}10^{-3}$ M upon 7 days of contact time. The spectra of both CSH gels before and after contact with Isa are shown in Fig. 3. Before contact with Isa, the spectra show the main peak of the CSH phase at approximately 950–970 cm^{-1}, which is related to Si-O-Si stretching vibrations (υ3 SiO4 or υ3 Si-O). This peak presents a small shift to high wavenumbers when the Ca/Si decreases. Other bands at 450–500 cm^{-1} and 665–667 cm^{-1} are also characteristic of SiO_4 tetrahedron vibrations. The peak at 818 cm^{-1} is more visible in the CSH phases with high Ca/Si, which show a higher degree of crystallinity (Fernández-Carrasco et al. [5]). The other spectral broad bands in the region of 3700–3000 cm^{-1}, with maxima close to 3450 cm^{-1}, and 1640 cm^{-1} correspond to structural hydroxyls and the H-O-H stretching vibrations of water.

Upon contact with Isa, the spectra clearly present peaks not existing in the original CSH gels. In both phases, but more clearly in CSH(1.4), an enhancement of peaks in the 1407–1413 cm^{-1} range is observed. The other two peaks appear at approximately 716 cm^{-1} and 871–873 cm^{-1} and are more pronounced in CSH(1.4). Finally, a shoulder at approximately 1050–1070 cm^{-1} appears in both CSHs. These peaks not observed in the reference samples confirm the existence of Isa/CSH interactions, the major effect of Isa being on the CSH gel with the higher Ca/Si ratio.

3.4. Adsorption of Ni on CSH in the presence of Isa

Fig. 4 shows the logarithm of the distribution coefficients of Ni, Log (K_d(Ni)), in the CSH as a function of the initial Isa concentration. The increase in Isa in the system leads to a moderate adverse effect on Ni sorption, with a decrease in the distribution coefficient in both CSH gels of a factor of 4–5. At the highest concentration of the organic ($1{\cdot}10^{-2}$ M), the log(K_d(Ni)) in the CSH (0.8) decreased from approximately 3.8 to 3.2 (K_d(Ni) from 6300 to 1600 $mL{\cdot}g^{-1}$) and in CSH(1.4) from 2.9 to 2.2 (K_d(Ni) from 794 to 158 $mL{\cdot}g^{-1}$).

4. Modelling and discussion

4.1. Ni and Isa speciation

To calculate the speciation of Isa and Ni, the specific pH and aqueous Ca content of the two analysed CSH suspensions were accounted for (Paragraph 3.1). The concentration of Ni was fixed to $1{\cdot}10^{-9}$ M and the concentration of Isa to $1{\cdot}10^{-4}$ M.

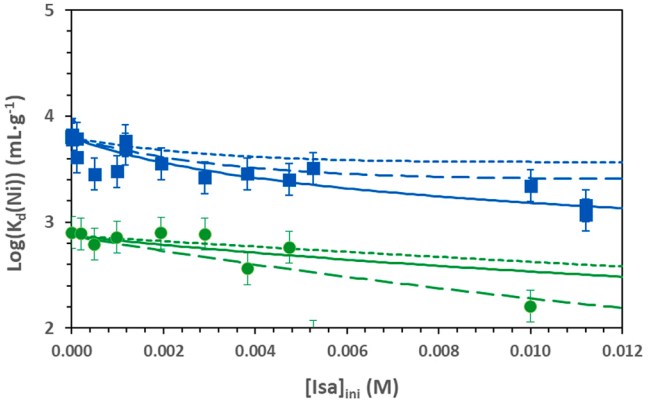


Fig. 4. Logarithm of Ni distribution coefficient *vs.* initial Isa concentration. Squares correspond to CSH(0.8), and circles correspond to CSH(1.4) (10 $g{\cdot}L^{-1}$). The lines correspond to the modelling of the distribution coefficients. Continuous line: no adsorption of Isa on the CSH; dotted line: Isa adsorption only in the weak site; dashed line: Isa adsorption on strong and weak sites.

The thermodynamic data for Isa complexes with Ni are summarised in Table 1, comparing the original OECD-NEA database in the ThermoChimie (TC) and the data after the revision of González-Siso (2018) (GS).

Complexes of Isa with calcium, the ion determining the potential of the CSH, are also included. The main species considered by the code is Isa[-]. For the Ni+Isa system, with respect to the original database (see Table 1), GS postulated a change in the formation constant of the species $Ni(OH)_3(Isa)^{2-}$ (LogK from −26.5 to −31) and proposed the existence of two additional Ni+Isa complexes.

Fig. 5 shows the results of the calculations for Isa speciation under the chemical conditions generated by the two CSH gels, expressed in % of the total organic. The major species is the anionic Isa^- in both CSH (0.8) and CSH(1.4), with concentrations of approximately 95% and 70%, respectively. Complexes with Ca, neutral Ca(Isa)(aq) and cationic $Ca(Isa)^+$ exist in non-negligible concentrations in CSH(1.4) (14%), whereas they are present in CSH(0.8) only to a lesser extent (<5%).

At the highest concentration of Isa (~$1{\cdot}10^{-2}$ M), the concentration of Isa-Ca complexes is approximately 13% and 24% of the total aqueous Ca for CSH(0.8) and CSH(1.4), respectively.

According to the speciation, the experimentally observed lowering of the ζ-potential of the CSH gels in the presence of Isa (Fig. 1) could then be produced by the complexation of Isa with Ca, which reducing aqueous Ca^{2+} also reduces the surface charge. Adsorption of the major anionic species (Isa^-) on the solid, may also reduce the surface charge, thus both processes will be analysed.

For what concerns the interactions of Isa with Ni, Table 2 summarises the results of the calculation of Ni speciation in the presence of Isa, expressed in % of total Ni for both CSH(0.8) and CSH(1.4). Calculations were performed using the data in Table 1 and considering the two databases (TC and GS) for comparison.

The revised GS database provides significant differences for Ni aqueous speciation, as discussed elsewhere [16] and, as can be observed in Table 2, also for Ni-Isa complexation. Nevertheless, both databases predict a relatively small quantity of Ni complexed with Isa (<6%). The relatively limited Ni-Isa complexation agrees with the moderate effect observed on Ni adsorption due to the presence of Isa (Fig. 4).

4.2. Sorption modelling

The analysis of the effects produced by the presence of Isa on Ni adsorption has been carried out considering a) only the aqueous Ni-Isa complexation and b) the contribution of Isa adsorption on the solids (on weak and strong sites). The effects of the increasing Isa content on Ni adsorption and on the CSHs surface charge were both analysed.

First, the calculation for Ni adsorption on CSH in the presence of Isa, was carried out considering only Ni-Isa aqueous complexes formation. The equations of the model described in paragraph 2.6 and the thermodynamic data of GS (Table 1) were used. The concentration of Ni was fixed to $1{\cdot}10^{-9}$ M, and the concentration of Isa was varied from $1{\cdot}10^{-5}$ to $1.2{\cdot}10^{-2}$ M. The corresponding pH and aqueous Ca content of each CSH suspension were accounted for in the calculations.

Table 1
Thermodynamic data for Isa complexes with Ni and other cations of interest. Basis species: Isa[-]. TC= [13]; GS= González-Siso (2018).

Species	Composition (CHESS code)	TC LogK	GS LogK
$Ca(Isa)_2$(cr)	1 Ca[2 +], 2 Isa[-]	6.4	6.4
Ca(Isa) [+]	1 Ca[2 +], 1 Isa[-]	1.7	1.7
Ca(Isa)(aq)	1 Ca[2 +], − 1 H[+], 1 Isa[-]	-10.4	-10.4
HIsa(aq)	1 H[+],1 Isa[-]	4	4
Ni(Isa) [+]	1 Ni[2 +], 1 Isa[-]	2.8	2.8
$Ni(OH)_3$(Isa) [2-]	1 Ni[2 +], 1 Isa[-], 3 H_2O, − 3 H[+]	**-26.5**	**-31**
$Ni(OH)_2$(Isa) [-]	1 Ni[2 +], 1 Isa[-], 2 H_2O, − 2 H[+]	–	**-17.6**
Ni(OH)(Isa)	1 Ni[2 +], 1 Isa[-], 1 H_2O, − 1 H[+]	–	**-6.5**

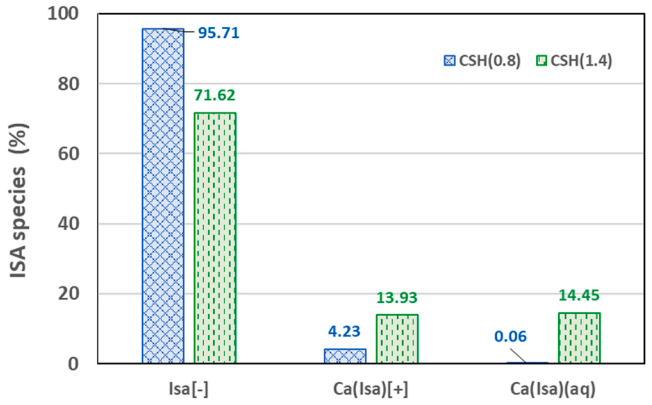


Fig. 5. Isa speciation in CSH waters expressed as a % of total ISA. Only the species with a percentage higher than 0.05% are shown. [Isa]= $1{\cdot}10^{-4}$ M.

Table 2
Calculation of Ni speciation in the presence of Isa for the two CSH phases. The results obtained considering the two databases: TC and GS. [Ni]= $1{\cdot}10^{-9}$ M and [Isa] to $1{\cdot}10^{-4}$ M.

(%)	CSH (0.8)		CSH (1.4)	
	TC	GS	TC	GS
Ni [2 +]	0.31	8.26	< 0.05	< 0.05
Ni(OH) [+]	1.44	38.71	< 0.05	1.12
$Ni(OH)_2$(aq)	90.08	48.36	11.96	94.00
$Ni(OH)_3$ [-]	7.55	< 0.05	82.07	3.89
Ni_2OH [3 +]	< 0.05	< 0.05	< 0.05	< 0.05
Ni(Isa) [+]	< 0.05	0.40	< 0.05	< 0.05
Ni(OH)(Isa)(aq)	–	3.65	–	0.06
$Ni(OH)_2$(Isa) [-]	–	0.58	–	0.85
$Ni(OH)_3$(Isa) [2-]	0.61	< 0.05	5.96	0.07
Σ(Ni-Isa)	**0.62**	**4.64**	**5.96**	**0.99**

The calculated $LogK_d$(Ni) values are superimposed on the experimental points as a continuous line (Fig. 4). As shown in the figure, the decrease in Ni sorption as a function of Isa concentration is satisfactorily predicted in both CSH phases. This result indicates that the Ni complexation with Isa in the aqueous phase, is probably the main mechanism responsible for Ni sorption decrease in the presence of the organic.

The variation of the surface potential derived from the presence of Isa and its aqueous complexation with Ca^{2+} is also plotted as a continuous line in Fig. 1. In this case, calculations slightly overestimate the experimental points in both CSH gels.

Then, to account for the possible contribution of Isa adsorption on the CSH phases and considering that the mayor Isa species in solution is the negatively charged Isa^-, the formation of the following additional complex to (a-d) can be proposed:

e) Surface complexation of Isa^-: $SiOCa^+ + Isa^- \leftrightarrow SiOCaIsa$

This equation can be written both for strong and weak sites of the CSH phases.

The LogK of this reaction in the weak sites, could be determined by comparing the experimental Kd(Isa) values with the calculated ones; in fact, sorption experiments with Isa on the CSH were carried out at relatively high Isa concentration.

If a value of LogK(weak) = −2.05 is fixed (Table S4) the calculated K_d(Isa) values are 65 $mL{\cdot}g^{-1}$ for CSH(0.8) and 94 $mL{\cdot}g^{-1}$ for CSH(1.4), in very good agreement with the experimental data. The Isa sorption behaviour, calculated as a function of Isa concentration, is shown in Fig. 2. The continuous line shows the calculation of K_d(Isa) ([Isa]= $1{\cdot}10^{-5}$ M to $1{\cdot}10^{-2}$ M) considering only the contribution of the weak site, directly determined by the experimental data. Within the range investigated, Isa adsorption shows a Langmuir-type behaviour and K_d(Isa) will decreases for concentrations above $1{\cdot}10^{-3}$ M.

The calculated $LogK_d$(Ni), taking into account Isa adsorption on CSH's weak sites is plotted in Fig. 4 as a dotted line. Similarly, the effect on the ζ-potential is plotted as a dotted line in Fig. 1.

From the experimental Isa adsorption data alone, it is not possible to isolate the contribution of Isa adsorption on strong sites. Isa adsorption on the strong sites is not expected to affect ζ-potential data either. Therefore, for evaluating more in depth this possible contribution, the information in Fig. 4 is the unique available.

A modelling exercise, detailed in the Supplementary Material, allowed determining the best value for LogK(strong) for Equation (e) needed to better reproduce the data in Fig. 4, for both CSH(0.8) and CSH (1.4) (Table S4.).

The calculated $LogK_d$(Ni) and the calculated ζ-potential obtained taking into account Isa adsorption considering the contribution of weak and strong sites are plotted in Fig. 4 and Fig. 1 as a dashed line.

The inclusion of Isa adsorption in the strong sites, as expected, does not affect neither the ζ- potential curves (Fig. 1) nor Isa adsorption isotherm within the range of interest (Fig. 2).

In general, the inclusion in the model of Isa adsorption provides only a small improvement of the fit to the experimental points. The difference observed in the simulations considering Isa adsorption or not remains contained within the experimental uncertainty range. Thus, adsorption of Isa in the CSH phases, seems to be less relevant than the formation of the Ni-Isa aqueous species on the overall behaviour of the system. In fact, the formation of the Ni-Isa aqueous species alone, represents quite well the decrease of Ni adsorption as ISA concentration increases.

Lastly, the possible formation of ternary CSH-Isa-Ni complexes cannot be ruled out *apriori*. Nevertheless, their presence is expected to improve Ni retention in the system and this effect is not experimentally seen. Furthermore, having observed the limited effect of Isa adsorption in the solids, a significant contribution on Ni adsorption due to the formation of ternary complexes can be discarded.

5. Conclusions

The presence of ISA at a concentration up to $1{\cdot}10^{-2}$ M slightly decreased the surface charge (−10 mV) of the two CSH phases analysed and moderately affected Ni adsorption, causing a diminution of K_d(Ni) by less than 1 order of magnitude.

The behaviour of the Ni/Isa/CSH ternary system could be well simulated using sorption modelling and considering the recently available thermodynamic data for Ni and Ni/Isa speciation. The formation of aqueous complexes of ISA with Ca, the ion determining the potential of the CSH phases and Ni, is the main factor responsible for the observed effects regarding both the solid surface charge and Ni adsorption reduction. The contribution of Isa adsorption on the CSH gels to the overall Ni retention behaviour is less relevant than the formation of the aqueous complexes.

Surface complexation modelling has been shown to be very useful for interpreting the behaviour of the ternary RN/organic/CSH system. As a support of improved sorption modelling–which is a very promising tool for predicting radionuclide behaviour under variable conditions–the relevance of maintaining updated thermodynamic databases, including new data under alkaline conditions, must be emphasised.

CRediT authorship contribution statement

Tiziana Missana Funding acquisition, Conceptualization, Investigation, Formal analysis, Validation, Writing – original draft, Writing – review & editing. **Miguel Garcia** Conceptualization, Investigation, Formal analysis, Resources. **Ursula Alonso** Conceptualization, Investigation, Formal analysis, validation, Writing – review & editing. **Ana María Fernandez** Investigation, Formal analysis, Resources.

Declaration of Competing Interest

The authors declare that they have no known competing financial interests or personal relationships that could have appeared to influence the work reported in this paper.

Data Availability

Data will be made available on request.

Acknowledgements

This study was partially supported by the European Union's Horizon 2020 Research and Innovation Programme under Grant Agreement no. 847593 (EURAD, CORI) and by the Spanish Ministry of Science and Innovation (PID2019–106398 GB-I00, ARNO Project). The personnel of the Division of Chemistry of CIEMAT are acknowledged for their support in chemical analyses.

Appendix A. Supporting information

Supplementary data associated with this article can be found in the online version at doi:10.1016/j.jece.2022.108500.

References

[1] J. Androniuk, C. Landesman, P. Henocq, A. Kalinichev, Adsorption of gluconate and uranyl on C-S-H phases: Combination of wet chemistry experiments and molecular dynamics simulations for the binary systems, Phys. Chem. Earth Parts A/B/C. 99 (2017) 194–203.

[2] H.B. Bradl, Adsorption of heavy metals ions on solid and solid constituents, J. Colloids Interface Sci. 277 (2004) 1–18.

[3] H. Brinkmann, M. Patzschke, P. Kaden, M. Raiwa, A. Rossberg, R. Klodiz, K. Heim, H. Moll, T. Stumpf, Complex formation between UO22+ and α-isosaccharinic acid: insight on a molecular level, Dalton Trans. 48 (2019) 13440.

[4] A.R. Brosi, C.J. Borkowski, E.E. Conn, J.C. Griess Jr, Characteristics of Ni-59 and Ni-63, Phys. Rev. 81 (3) (1951) 391–395, https://doi.org/10.1103/PhysRev.81.391.

[5] Fernández-Carrasco L., Torrens-Martín D., Morales L.M. and Martínez-Ramírez S. (2012). Infrared Spectroscopy in the Analysis of Building and Construction Materials, Infrared Spectroscopy - Materials Science, Engineering and Technology, ISBN: 978–953-51–0537-4.

[6] H. Gamsjäger, J. Bugajzki, T. Gajda, R.J. Lemire, W. Preis, Chemical thermodynamics of Nickel. Chemical Termodynamics, in: OECD-NEA, Vol 6, Elsevier,, 2005.

[7] D. García, P. Henocq, O. Riba, M. López-García, B. Madé, J.C. Robinet, Adsorption behaviour of isosaccharinic acid onto cementitious materials, Appl. Geochem 118 (2020), 104625.

[8] E. Giffaut, M. Grivé, Ph Blanc, Ph Vieillard, E. Colás, H. Gailhanou, S. Gaboreau, N. Marty, B. Madé, L. Duro, Andra thermodynamic database for performance assessment: ThermoChimie, Appl. Geochem. 49 (2014) 225–236.

[9] M.A. Glaus, L.R. van Loon, Degradation of cellulose under alkaline conditions: new insights from a 12 years degradation study, Environ. Sci. Technol. 42 (2008) 2906–2911.

[10] M.R. González-Siso, X. Gaona, L. Duro, M. Altmaier, J. Bruno, Thermodynamic model of Ni(II) solubility, hydrolysis and complex formation with ISA, Radiochim. Acta 106 (2018) 31–45, https://doi.org/10.1515/ract-2017-2762.

[11] B. Grambow, M. López-García, J. Olmeda, M. Grivé, N.C.M. Marty, S. Grangeon, F. Claret, S. Lange, G. Deissmann, M. Klinkenberg, D. Bosbach, C. Bucur, I. Florea, R. Dobrin, M. Isaacs, D. Read, J. Kittnerová, B. Drtinová, D. Vopálka, N. Cevirim-Papaioannou, N. Ait-Mouheb, X. Gaona, M. Altmaier, L. Nedyalkova, B. Lothenbach, J. Tits, C. Landesman, S. Rasamimanana, S. Ribet, Retention and diffusion of radioactive and toxic species on cementitious systems: main outcome of the CEBAMA project, Appl. Geochem. (2020) 112, https://doi.org/10.1016/j.apgeochem.2019.104480.

[12] A.M. Harrison, *in* Lea's chemistry of cement and concrete (Fifth Edition), Const. Specif. Portland Cem. (2019) 87–155.

[13] Hummel, W., Anderegg, G., Rao, L., Puigdomènech, I., Tochiyama, O. (2005). Chemical Thermodynamics of Compounds and Complexes of U, Np, Pu, Am, Tc, Se, Ni and Zr with selected Organic Ligands. Chemical Termodynamics Vol 9., 1088 pag, OECD-NEA, Elsevier.

[14] M.J. Keith-Roach, The speciation, stability, solubility and biodegradation of organic cocontaminant radionuclide complexes: a review, Sci. Total Environ. 396 (2008) 1–11, https://doi.org/10.1016/j.scitotenv.2008.02.030.

[15] G. Kuippers, C. Boothman, H. Bagshaw, M. Ward, R. Beard, N. Bryan, J.R. Lloyd, The biogeochemical fate of nickel during microbial ISA degradation; Implications for nuclear waste disposal, Sci. Rep. 8 (2018) 1–11, https://doi.org/10.1038/s41598-018-26963-8.

[16] T. Missana, M. García-Gutiérrez, U. Alonso, O. Almendro-Ginestá, Nickel retention by calcium silicate hydrate phases: Evaluation of the role of the Ca/Si ratio on adsorption and precipitation processes, Appl. Geochem. (2022), 105197, https://doi.org/10.1016/j.apgeochem.2022.105197.

[17] T. Missana, M. García-Gutiérrez, M. Mingarro, U. Alonso, Analysis of barium retention mechanisms on calcium silicate hydrate phases, Cem. Concr. Res. 93 (2017) 8–16, https://doi.org/10.1016/j.cemconres.2016.12.004.

[18] M. Ochs, F. Dolder, Y. Tachi, Decrease of radionuclide sorption in hydrated cement systems by organic ligands: Comparative evaluation using experimental data and thermodynamic calculations for ISA/EDTA-actinide-cement systems, Appl. Geochem. 136 (2021), 105161, https://doi.org/10.1016/j.apgeochem.2021.105161.

[19] I. Pavasars, J. Hagberg, H. Borén, B. Allard, Alkaline degradation of cellulose: mechanisms and kinetics, J. Polym. Environ. 11 (2003) 39–47, https://doi.org/10.1023/A:1024267704794.

[20] P.H. Santschi, C. Xu, S. Zhang, K.A. Schwehr, P. Lin, C.M. Yeager, D.I. Kaplan, Recent advances in the detection of specific natural organic compounds as carriers for radionuclides in soil and water environments, with examples of radioiodine and plutonium, J. Environ. Radio. 171 (2017) 226–233, https://doi.org/10.1016/j.jenvrad.2017.02.023.

[21] D.L. Sparks, Toxic metals in the environment: the role of surfaces, Elements 1 (2005) 193–197.

[22] Van der Lee J. and de Windt L. CHESS tutorial and cookbook (1999). Technical Report LHM/RD/99/05.

[23] Van Loon L.R. and Glaus M.A. (1998). Experimental and theoretical studies on alkaline degradation of cellulose and its impact on the sorption of radionuclides. PSI Bericht Nr 98–07 or Nagra TR 97–04.

[24] P. Warwick, N. Evans, S. Vines, Studies on some divalent metal α-isosaccharinic acid complexes, Radiochim. Acta 94 (2006) 363–368.